Communication

Microstrip-Fed Surface-Wave Antenna for Endfire Radiation

Yuefeng Hou, Yue Li, Zhijun Zhang, and Magdy F. Iskander

***Abstract*— This communication presents a microstrip-fed surface-wave antenna for endfire radiation. The antenna has the advantages of high endfire gain, wide endfire gain bandwidth, and stable endfire radiation pattern. It consists of a microstrip line with air media and a dielectric cuboid. The half-mode dielectric waveguide, which is made up by the dielectric cuboid and the air substrate introduced by the microstrip line, is the radiating structure of the antenna. Fed by a microstrip line, the half-mode dielectric waveguide couples the energy continuously with a moderate phase constant, which is helpful for the antenna to realize a high endfire gain and a stable endfire radiation pattern. With a low dielectric constant, the half-mode dielectric waveguide has a stable radiation performance within a wide bandwidth. With a length of 5.76 wavelength, the antenna achieves a maximum endfire gain of 13.3 dBi at 4.75 GHz. The 1 and 3 dB gain bandwidths of the antenna is 18.1% and 37.8%, respectively. Good matching is obtained from 3 to 6.5 GHz.**

***Index Terms*— Endfire, high endfire gain, large conducting plane, stable radiation pattern, surface-wave antenna, wide gain bandwidth.**

I. Introduction

In recent years, more and more attentions have been paid to the endfire antennas mounted on a large conducting plane due to their applications on the unmanned aerial vehicle, missile [1], and reconnaissance vehicle. Although multiple antennas with the performance of low profile, wideband, high front-to-back ratio, and high gain have been extensively investigated, the bandwidth of endfire gain needs to be improved. Moreover, it is still a great challenge to realize an endfire antenna mounted on a large conducting plane with the advantages of high endfire gain, wide endfire gain bandwidth, and stable endfire radiation pattern simultaneously.

Due to the problems of short radiating structure or nonuniform energy distribution on the radiating aperture, many endfire antennas mounted on a large conducting plane have a low endfire gain and sloping-upward main-beam direction. For example, in the open literature, Yagi array antennas [2]–[8] and horn antennas [9], [10] have the radiating structure with the length less than 3.5 wavelength at the center frequency. When the Yagi array antenna is designed with a long radiating structure, the director element couples less energy from the space when it is far away from the driven element. Therefore, the increase of the director element number will have weaker influence on the endfire gain, which leads to gain reduction [11]. For the logperiodic arrays [12]–[14] and surface-wave antennas [15]–[16], only part radiating aperture of the antennas radiates energy at single-frequency point, which decreases the endfire gain.

For the endfire antennas mounted on a large conducting plane with a long radiating structure, they have the problems of unstable radiation pattern because of the unsuitable propagate mode or narrow gain bandwidth because of the resonant nature. For example, the SIW leaky-wave antennas in [17] and [18] work on waveguide modes, which lead to the beam direction changing drastically versus frequency. Fed by microstrip line with air media, the leaky-wave antennas [19], [20] have a moderate phase constant and could achieve a stable endfire radiation pattern with high endfire gain. However, due to the resonant feature of radiating structures, the endfire gain bandwidths of the antennas are relatively narrow.

In this communication, a microstrip-fed surface-wave antenna is presented. The proposed antenna consists of a microstrip line with air media and a dielectric cuboid. The dielectric cuboid and the air substrate introduced by the microstrip line make up a half-mode dielectric waveguide. The half-mode dielectric waveguide is the radiating structure of the proposed antenna, and it radiates the energy by surface wave. Designed with a low dielectric constant and fed by a microstrip line with air media, the proposed antenna achieves a good radiation performance for the following reasons.

1) The radiation performance of the antenna is stable.
2) The radiating aperture distribution of the antenna is improved.
3) The antenna could be designed with a long structure readily.
4) The antenna has a moderate and stable phase constant.

Finally, a prototype is designed and fabricated. The measured results show that the proposed antenna has the advantages of high endfire gain, wide endfire gain bandwidth, and stable endfire radiation pattern.

II. Antenna Design and Analysis

The proposed antenna is a multilayered structure which consists of a microstrip line with air media and a dielectric cuboid. The copper strip and the copper sheet make up the microstrip line with air media, as presented in Fig. 1(b). To mitigate the effect of the discontinuities between the microstrip line and the coaxial lines, tapered structures are added between them.

The proposed antenna adopts a dielectric cuboid as the radiating structure, which is different from the traditional dielectric waveguide antennas with a tapered structure [21], [22]. The configuration of the dielectric cuboid is shown in Fig. 1(a). The dielectric cuboid and the air layer introduced by the microstrip line form a half-mode dielectric waveguide which works on TM_0 odd mode [23]. In [15], it is concluded that when the half-mode dielectric waveguide is made up by a lower dielectric constant material, it has a more stable performance. In [24], it is concluded that the dielectric ohmic losses would reduce the radiation efficiency of the proposed antenna. Therefore, the dielectric cuboid is made up by the Teflon, which is a low dielectric constant and low dielectric loss material (permittivity of 2.1 and loss tangent of 0.002), to realize a stable performance and a good radiation efficiency.

The analysis in [15] presents that when the half-mode dielectric waveguide has the height of $\lambda/4\sqrt{\varepsilon_r}$, it could radiate the energy to free space effectively. ε_r is the dielectric constant of the half-mode dielectric waveguide. The width of the half-mode dielectric waveguide influences the beamwidth in the H-plane. Therefore,

Manuscript received May 5, 2018; revised August 24, 2018; accepted September 3, 2018. Date of publication October 9, 2018; date of current version January 16, 2019. This work was supported by the National Natural Science Foundation of China under Contract 61525104. *(Corresponding author: Zhijun Zhang.)*

The authors are with the Beijing National Research Center for Information Science and Technology, Tsinghua University, Beijing 100084, China (e-mail: zjzh@tsinghua.edu.cn).

Color versions of one or more of the figures in this communication are available online at http://ieeexplore.ieee.org.

Digital Object Identifier 10.1109/TAP.2018.2874713

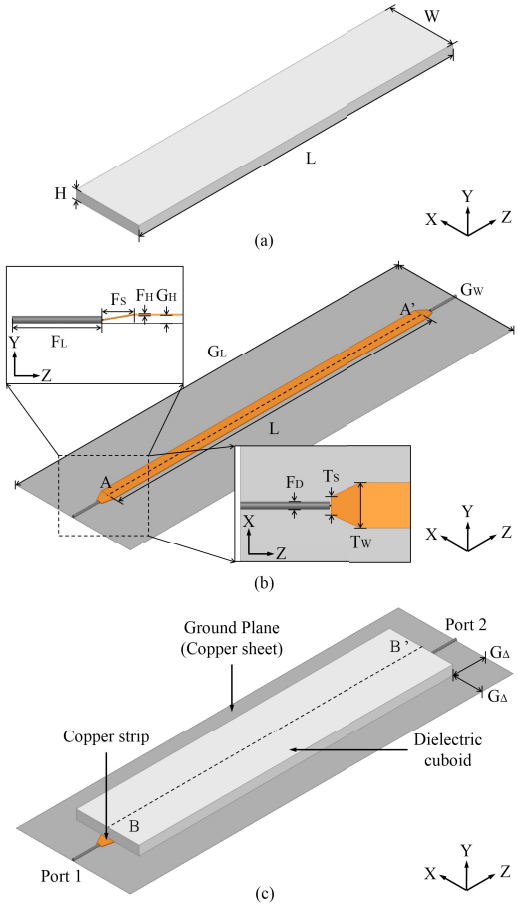

Fig. 1. Configuration of the proposed microstrip-fed surface-wave antenna. (a) Dielectric cuboid. (b) Microstrip line with air media. (c) Entire antenna.

TABLE I
DETAILED DIMENSION OF THE PROPOSED ANTENNA

Parameter	Value (mm)	Parameter	Value (mm)
L	364	F_L	29.5
W	72.5	F_S	10
H	11	F_H	0.5
G_L	444	F_D	2
G_W	132	T_W	15
G_H	2.7	T_S	6

to realize a good radiation capacity and a suitable beamwidth, the height and the width of the dielectric cuboid are optimized. The detailed dimensions of the dielectric cuboid are given in Table I.

By clinging the dielectric cuboid to the top of the microstrip line, the proposed antenna is achieved and the configuration is shown in Fig. 1(c). Because the two structures exhibit similar modal field configurations, the half-mode dielectric waveguide could couple the energy from the microstrip line with only slightly influence on the reflection coefficient of the microstrip line, as shown in Fig. 2(a).

To explain the relationship between the two field configurations clearly, the vector electric field (E-field) distributions on the *yoz* plane through the reference lines *AA'* and *BB'* at the center frequency of 4.75 GHz are shown in Fig. 2(b) and (c), respectively. Reference lines of *AA'* and *BB'* are plotted in Fig. 1(b) and (c), respectively. As shown in Fig. 2(b), around the microstrip line with air media working on the TEM mode, all of the vector E-fields are perpendicular to the ground plane. The energy of the E-field almost concentrates

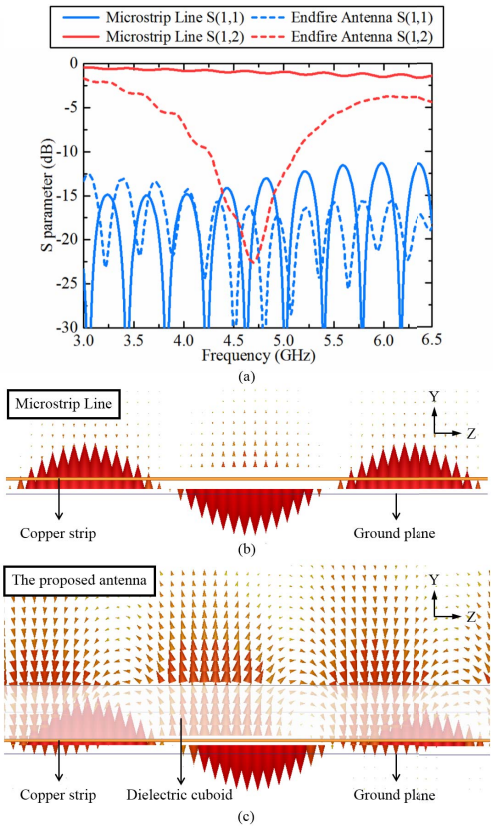

Fig. 2. Influence of the dielectric cuboid on the microstrip line. (a) S-parameters of the microstrip line with or without the dielectric cuboid. (b) and (c) Vector E-field distributions on the *yoz* plane through the reference lines *AA'* and *BB'* at the center frequency of 4.75 GHz, respectively.

in the microstrip line. Only a small part of energy exists above the microstrip line. The vector E-field in the microstrip line and above the microstrip line has the opposite direction. As shown in Fig. 2(c), part of the vector E-field in the dielectric cuboid, which is defined as $\overrightarrow{E_1}$, is parallel to the ground plane and points to the propagation direction. The maximum energy of $\overrightarrow{E_1}$ is located on the upper surface of the dielectric cuboid. The other part of the vector E-field in the dielectric cuboid, which is defined as $\overrightarrow{E_2}$, is perpendicular to the ground plane. The E-field $\overrightarrow{E_2}$ could stably exist close to the top of the microstrip line due to the boundary conditions. Therefore, because the TM_0 mode in the half-mode dielectric waveguide and the TEM mode in the microstrip line have the similar modal field configurations, the half-mode dielectric waveguide could gradually couple the energy in the microstrip line without disturbing the performance of the microstrip line seriously, which also indicates that the proposed antenna is suitable to be designed with a long structure.

From Fig. 2(b) and (c), the proposed antenna has two paths to propagate the energy, which is similar to the antenna in [20]. One of the paths is in the microstrip line, and the other path is in the half-mode dielectric waveguide. As shown in Fig. 3(a), because the whole half-node dielectric waveguide could couple the energy from the microstrip line, the E-field magnitude distribution in the microstrip line gradually decreases. However, the energy distribution in the dielectric cuboid is almost uniform. Therefore, comparing with the half-mode dielectric waveguide antennas in [15] and [16] which have only one propagation path, the proposed antenna could radiate the energy by the whole radiating aperture. Moreover, comparing with the theoretical model in [25] and [26] whose radiating aperture has exponentially decaying distribution, the proposed antenna has a

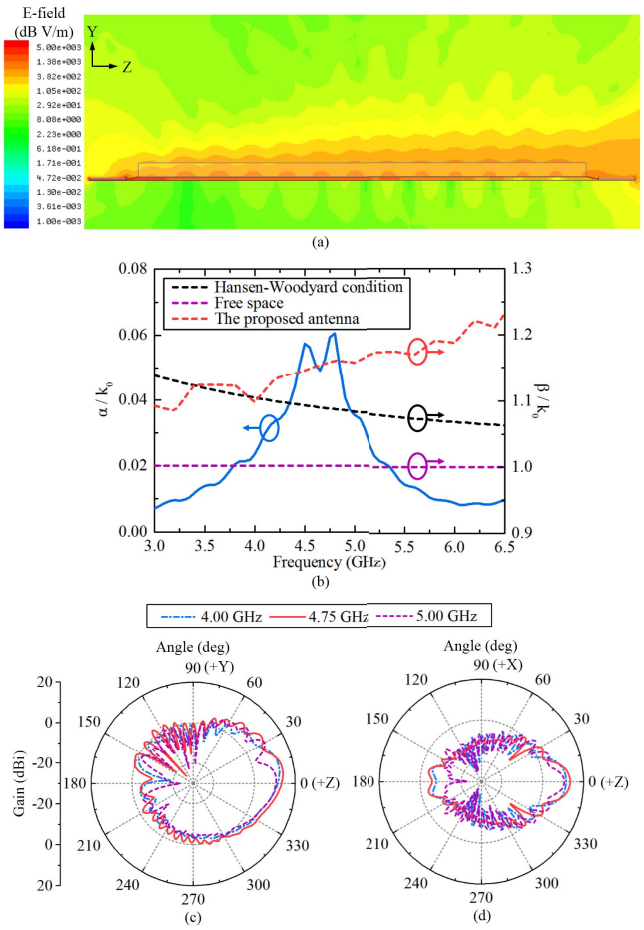

Fig. 3. Performance of the proposed antenna. (a) E-field magnitude distribution on the yoz plane through the reference line BB'. (b) Normalized leakage constant and normalized phase constant of the proposed antenna versus frequency. (c) and (d) Simulated radiation patterns of the proposed antenna at different frequencies in the E-plane (yoz plane) and the H-plane (xoz plane), respectively.

more uniform radiating aperture distribution, which improves the endfire gain.

Because the microstrip line of the proposed antenna has an air substrate and all of the microstrip lines are designed by copper, the ohmic loss introduced by the microstrip line is small. Therefore, the leakage constant extracted from the simulated model [27] is mainly determined by the coupling ability of the half-mode dielectric waveguide. Part of the energy in the half-mode dielectric waveguide is lost due to the dielectric loss, and the other is radiated to free space. As shown in Fig. 3(b), when the half-mode dielectric waveguide couples more energy from the microstrip line, a higher leakage constants is achieved.

The half-mode dielectric waveguide obtains a moderate and stable phase constant when it is fed by the microstrip line with air media. The normalized phase constant versus the frequency is shown in Fig. 3(b). On the middle of the dielectric cuboid, the phase constant along the propagation direction is the phase constant of the proposed antenna [28]. As a comparison, the phase constant in free space and theoretical value calculated based on Hansen–Woodyard (H–W) condition [29] is presented in Fig. 3(b). It is found that the phase constant in the dielectric cuboid is close to the phase constant of H–W condition, which indicates that the proposed antenna has a good and stable endfire radiation pattern over a wide frequency band.

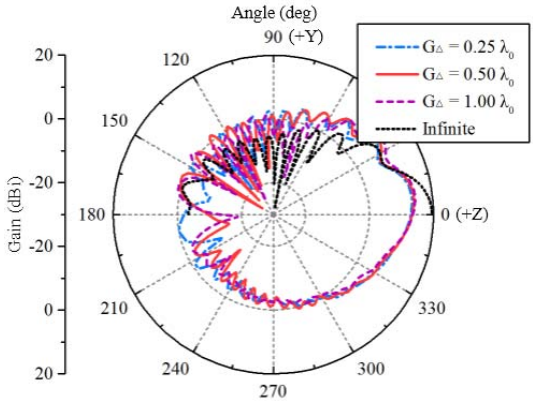

Fig. 4. Simulated radiation patterns at the center frequency of 4.75 GHz in the E-plane (yoz plane) with different G_D.

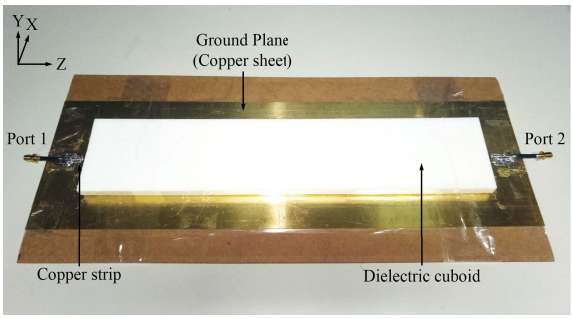

Fig. 5. Fabricated prototype of the proposed antenna.

The radiation patterns of the E-plane and the H-plane at different frequencies are presented in Fig. 3(c) and (d), respectively. Due to the influence of the finite ground, the beam directions are upward in the E-plane, as shown in Fig. 3(c). With the increasing of the frequency, the beam directions are closer to the endfire due to the increasing of the phase constant. The beam directions at 4, 4.75, and 5.5 GHz are 11°, 9°, and 3°, respectively. Meanwhile, with the increasing of the frequency, the beamwidth becomes narrower because the relative length of the radiating aperture increases, as shown in Fig. 3(d). Moreover, because the phase constant of the antenna increases, the normalized beamwidth and sidelobe level increase simultaneously, which satisfies the theoretical analysis about the beamwidth properties in [26]. The half-power beam width (HPBW) at 4, 4.75 and 5.5 GHz are 27°, 21°, and 17°, respectively. It is found that all of the front-to-back radios at the three frequency points are higher than 15 dB. From Fig. 3(c) and (d), a good and stable endfire radiation pattern is achieved by the proposed antenna over a wide bandwidth.

The radiation patterns of the proposed antenna with different sizes of the ground plane at the center frequency are shown in Fig. 4. With the dimension of the ground plane increasing, the value of the endfire gain and the front-to-back radio improves. The G_Δ is the distance between the edge of ground plane and the edge of the dielectric cuboid, as shown in Fig. 1(c). When the G_Δ changes from $0.25\lambda_0$ to $1\lambda_0$, the endfire gain increases from 12.91 to 13.56 dBi and the front-to-back radio increases from 15.2 to 26.6 dB. If the proposed antenna is designed with the infinite ground plane, the beam direction is endfire, as shown in Fig. 4. The endfire gain of the antenna with infinite ground plane is about 6 dB higher than the antenna with finite ground plane.

III. Experimental Results

A prototype is fabricated and measured to provide a verification of the new design method. Geometry of the corresponding microstrip-fed half-mode dielectric waveguide antenna is shown in Fig. 5.

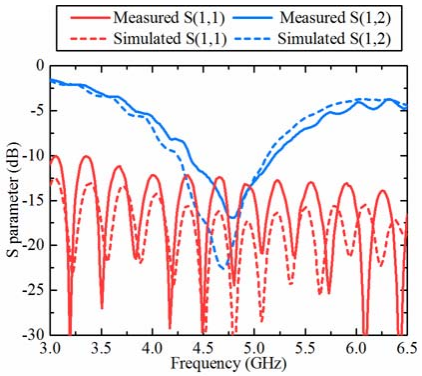

Fig. 6. Simulated and measured S-parameters of the proposed antenna.

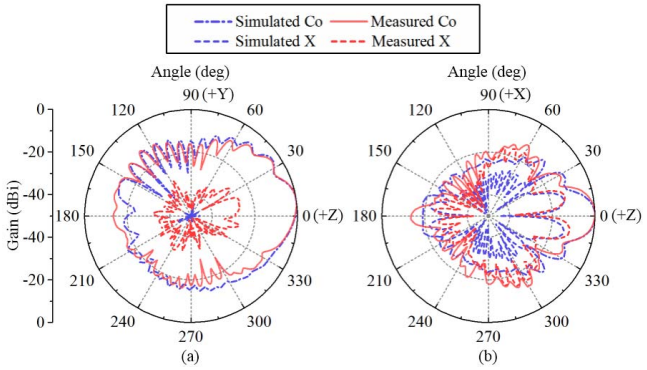

Fig. 7. Simulated and measured normalized radiation patterns of the proposed antenna at the center frequency of 4.75 GHz in (a) E-plane (*yoz* plane) and (b) H-plane (*xoz* plane).

The antenna is excited at the port 1. The port 2 is terminated with a match load. Four nylon columns are under the edges of dielectric cuboid to support the proposed antenna. S-parameters were measured using a N5071B vector network analyzer (300 kHz–9 GHz); the gains and radiation patterns were measured in a far-field anechoic chamber.

The simulated and measured S-parameters of the proposed antenna are shown in Fig. 6, verifying that good matching is achieved over the operating band from 3 to 6.5 GHz. The low level of the transmission coefficient indicates that high radiation efficiency of the antenna. The transmission magnitude is lower than −15 dB at the center frequency of 4.75 GHz. The simulated and measured normalized radiation patterns of the E-plane and the H-plane at the center frequency are shown in Fig. 7. Due to the existence of the finite ground plane, the radiation beam angle in the E-plane is about 9° away from the endfire direction as shown in Fig. 7(a). In the H-plane, the HPBW of the radiation pattern is nearly 23° as shown in Fig. 7(b). The proposed antenna has a high level of front-to-back radio and a low level of crosspolarization. The front-to-back radio is 18.6 dB, and the crosspolarization is about 28 dB lower than copolarization at the center frequency. Fig. 8 shows the simulated and measured endfire gains of the antenna. The measured endfire gain of the proposed antenna is better than 10 dBi from 3.75 to 5.65 GHz with a maximum value of 13.3 dBi at the center frequency of 4.75 GHz. The measured 1 and 3 dB gain bandwidths can reach 18.1% and 37.8%, respectively. Good agreement between the measurement and the simulation has been obtained.

Table II shows a comparison between existing designs in the literature and the proposed antenna. The performances of the antennas are presented at the frequency when the antennas achieve the maximum endfire gain. λ_0 is the wavelength in free space at the frequency when the antennas achieve the maximum endfire gain. ε_r is the dielectric constant of the material filling the antenna. Comparing with the endfire antennas mounted on a large conducting plane which explicitly presents the endfire gain versus the frequency, it is found that the proposed antenna provides a relatively higher endfire gain and a wider gain bandwidth.

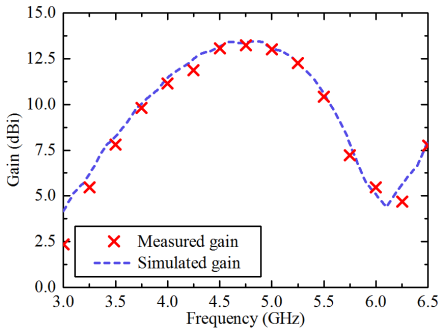

Fig. 8. Simulated and measured endfire gains of the proposed antenna.

TABLE II
COMPARISON OF DIMENSIONS AND ENDFIRE GAIN AMONG ANTENNAS WITH ENDFIRE RADIATION

Reference	Length (λ_0)	Dielectric (ε_r)	Maximum Endfire Gain (dBi)	-1dB Gain BW (%)	-3dB Gain BW (%)
[11]	2.97	2.33	10.4	3.7	7.6
[14]	2.41	2.1	9.7	7.9	15.8
[19]	6.10	1	11.5	4.0	7.0
[20]	5.67	1	13.3	8.0	17.0
Proposed antenna	5.76	2.1	13.3	18.1	37.8

IV. CONCLUSION

This communication proposes a microstrip-fed surface-wave antenna for endfire radiation. The proposed antenna has two paths to propagate the energy. Therefore, the half-mode dielectric waveguide, which is the radiating structure of the antenna, obtains a relative uniform aperture distribution. Fed by the microstrip line with air media, the half-mode dielectric waveguide achieves a moderate and stable phase constant. By adopting a low dielectric constant, the half-mode dielectric waveguide has a stable radiation performance over a wide frequency band. Therefore, the antenna has a good performance in endfire gain, endfire gain bandwidth, and endfire radiation pattern. The proposed antenna is suitable for the wideband long-distance communication. It also has a potential in conformal and platform-embedded applications.

REFERENCES

[1] Y. Xia, B. Muneer, and Q. Zhu, "Design of a full solid angle scanning cylindrical-and-conical phased array antennas," *IEEE Trans. Antennas Propag.*, vol. 65, no. 9, pp. 4645–4655, Sep. 2017.

[2] A. Y. Simba, M. Yamamoto, and K. Itoh, "Planar-type sectored antenna based on slot Yagi-Uda array," *IEE Proc.–Microw., Antennas Propag.*, vol. 152, no. 5, pp. 347–353, 2005.

[3] P. Rodriguez-Ulibarri and T. Bertuch, "Microstrip-fed complementary Yagi-Uda antenna," *IET Microw., Antennas Propag.*, vol. 10, no. 9, pp. 926–931, 2016.

[4] Z. Liang, J. Liu, Y. Zhang, and Y. Long, "A novel microstrip quasi Yagi array antenna with annular sector directors," *IEEE Trans. Antennas Propag.*, vol. 63, no. 10, pp. 4524–4529, Oct. 2015.

[5] G. R. DeJean and M. M. Tentzeris, "A new high-gain microstrip Yagi array antenna with a high front-to-back (F/B) ratio for WLAN and millimeter-wave applications," *IEEE Trans. Antennas Propag.*, vol. 55, no. 2, pp. 298–304, Feb. 2007.

[6] E. Guo, J. Liu, and Y. Long, "A mode-superposed microstrip patch antenna and its Yagi array with high front-to-back ratio," *IEEE Trans. Antennas Propag.*, vol. 65, no. 12, pp. 7328–7333, Dec. 2017.

[7] Z. Hu, Z. Shen, W. Wu, and J. Lu, "Low-profile top-hat monopole Yagi antenna for end-fire radiation," *IEEE Trans. Antennas Propag.*, vol. 63, no. 7, pp. 2851–2857, Jul. 2015.

[8] Y. Zhao, Z. Shen, and W. Wu, "Wideband and low-profile monocone quasi-Yagi antenna for end-fire radiation," *IEEE Antennas Wireless Propag. Lett.*, vol. 16, pp. 325–328, 2017.

[9] Y. Zhao, Z. Shen, and W. Wu, "Wideband and low-profile H-plane ridged SIW horn antenna mounted on a large conducting plane," *IEEE Trans. Antennas Propag.*, vol. 62, no. 11, pp. 5895–5900, Nov. 2014.

[10] Y. Zhao, Z. Shen, and W. Wu, "Conformal SIW H-plane horn antenna on a conducting cylinder," *IEEE Antennas Wireless Propag. Lett.*, vol. 14, pp. 1271–1274, 2015.

[11] J. Liu and Q. Xue, "Microstrip magnetic dipole Yagi array antenna with endfire radiation and vertical polarization," *IEEE Trans. Antennas Propag.*, vol. 61, no. 3, pp. 1140–1147, Mar. 2013.

[12] Z. Hu, Z. Shen, W. Wu, and J. Lu, "Low-profile log-periodic monopole array," *IEEE Trans. Antennas Propag.*, vol. 63, no. 12, pp. 5484–5491, Dec. 2015.

[13] Q. Chen, Z. Hu, Z. Shen, and W. Wu, "2-18 GHz conformal low-profile log-periodic array on a cylindrical conductor," *IEEE Trans. Antennas Propag.*, vol. 66, no. 2, pp. 729–736, Feb. 2018.

[14] S. Zhang and G. F. Pedersen, "Compact wideband and low-profile antenna mountable on large metallic surfaces," *IEEE Trans. Antennas Propag.*, vol. 65, no. 1, pp. 6–16, Jan. 2017.

[15] Z. Chen and Z. Shen, "Wideband flush-mounted surface wave antenna of very low profile," *IEEE Trans. Antennas Propag.*, vol. 63, no. 6, pp. 2430–2438, Jun. 2015.

[16] P. Wang and Z. Shen, "End-fire surface wave antenna with metasurface coating," *IEEE Access*, vol. 6, pp. 23778–23785, 2018.

[17] J. Liu, D. R. Jackson, and Y. Long, "Substrate integrated waveguide (SIW) leaky-wave antenna with transverse slots," *IEEE Trans. Antennas Propag.*, vol. 60, no. 1, pp. 20–29, Jan. 2012.

[18] J. Liu, D. R. Jackson, Y. Li, C. Zhang, and Y. Long, "Investigations of SIW leaky-wave antenna for endfire-radiation with narrow beam and sidelobe suppression," *IEEE Trans. Antennas Propag.*, vol. 62, no. 9, pp. 4489–4497, Sep. 2014.

[19] P. Liu, H. Feng, Y. Li, and Z. Zhang, "Low-profile endfire leaky-wave antenna with air media," *IEEE Trans. Antennas Propag.*, vol. 66, no. 3, pp. 1086–1092, Mar. 2018.

[20] Y. Hou, Y. Li, Z. Zhang, and Z. Feng, "Narrow-width periodic leaky-wave antenna array for endfire radiation based on hansen-woodyard condition," *IEEE Trans. Antennas Propag.*, to be published.

[21] D. H. Schaubert, E. L. Kollberg, T. Korzeniowski, T. Thungren, J. Johansson, and K. S. Yngvesson, "Endfire tapered slot antennas on dielectric substrates," *IEEE Trans. Antennas Propag.*, vol. AP-33, no. 12, pp. 1392–1400, Dec. 1985.

[22] K. S. Yngvesson, T. L. Korzeniowski, Y. S. Kim, E. L. Kollberg, and J. F. Johansson, "The tapered slot antenna-a new integrated element for millimeter-wave applications," *IEEE Trans. Mobile Comput.*, vol. 37, no. 2, pp. 365–374, Feb. 1989.

[23] C. A. Balanis, *Advanced Engineering Electromagnetics*, 2nd ed. Hoboken, NJ, USA: Wiley, 2011, p. 434.

[24] C. Di Nallo, F. Frezza, A. Galli, and P. Lampariello, "Rigorous evaluation of ohmic-loss effects for accurate design of traveling-wave antennas," *J. Electromagn. Waves Appl.*, vol. 12, no. 1, pp. 39–58, 1998.

[25] E. M. O'Connor, D. R. Jackson, and S. A. Long, "Extension of the hansen-woodyard condition for endfire leaky-wave antennas," *IEEE Antennas Wireless Propag. Lett.*, vol. 9, pp. 1201–1204, 2010.

[26] W. Fuscaldo, D. R. Jackson, and A. Galli, "Beamwidth properties of endfire 1-D leaky-wave antennas," *IEEE Trans. Antennas Propag.*, vol. 65, no. 11, pp. 6120–6125, Nov. 2017.

[27] J. L. Volakis, *Antenna Engineering Handbook*, 4th ed. New York, NY, USA: McGraw-Hill, 2007, pp. 7–11.

[28] D. M. Pozar, *Microwave Engineering*, 4th ed. Hoboken, NJ, USA: Wiley, 2011, p. 135.

[29] W. W. Hansen and J. R. Woodyard, "A new principle in directional antenna design," *Proc. IRE*, vol. 26, no. 3, pp. 333–345, Mar. 1938.